

Flow of Viscous Fluid Through a Circular Aperture

J. S. CHONG,* E. B. CHRISTIANSEN, and
A. D. BAER, *University of Utah, Salt Lake City, Utah 84112*

Synopsis

The creeping flow of a highly viscous incompressible fluid through a circular aperture located in an infinitely wide horizontal plate is analyzed by solving Navier-Stokes equations without inertia terms. Solutions for vertical and radial velocities as well as pressure have been obtained in terms of integral equations with an undetermined Kernal function. This function has been evaluated by assuming several different velocity distributions at the aperture, and the corresponding pressure drop for each case has been calculated. The results show that the pressure loss for a given flow rate goes through a minimum as the assumed velocity profile changes from flat to parabolic. Based on the minimum energy dissipation theorem of Helmholtz, the most appropriate velocity distribution is discussed. Experimental data obtained using sharp-edged orifices are compared with theoretical predictions.

INTRODUCTION

The creeping flow of a viscous Newtonian fluid through a thin circular aperture is of theoretical as well as practical interest in view of its novel application to determine viscosities of highly concentrated suspensions without the wall effect.¹ Furthermore, there is a need to separate the entrance pressure drop associated with viscous energy dissipation from the elastic effect for the flow of various polymer melts through cylindrical tubes.

Weissberg² calculated the end correction for slow viscous flow through a long tube based on the minimum energy dissipation theorem. His flow regions of interest lie in the semi-infinite space outside of the tube inlet as well as in the space between the inlet and the midsection of the tube where fluid velocity is fully developed. Under this condition he assumes that the rate of energy dissipation or the pressure drop is a function only of the vorticity. However, this vorticity must satisfy a velocity field governed by the creeping flow. Unfortunately, the trial stream function he used does not satisfy the vorticity equation, eq. (33).

Furthermore, his calculation shows that the pressure drop is not very sensitive to the form of the stream function he used. Roscoe³ obtained a relationship between pressure drop and flow rate for slow viscous flow through a

* Present address: E. I. du Pont De Nemours & Co., Inc., Photo Products Department, Parlin, New Jersey 08859.

circular aperture in which stream lines on the high and low pressure sides of the aperture are symmetrical. His method is based on the analogy with the electrical potential around a grounded, conducting thin plate. However, he did not give the details of the method by which the final solution was obtained.

The present work treats the creeping flow of a highly viscous Newtonian fluid through a thin aperture located in an infinitely wide plate above which the fluid stands and flows downward through the aperture into the atmosphere. Under this condition we find that the rate of energy dissipation cannot be calculated without knowing the velocity field at or above the aperture. Although we apply the minimum energy dissipation concept to obtain an approximate solution for the pressure drop, basically, the boundary value problem associated with the creeping flow into an aperture is ill defined and an exact solution cannot be obtained. In the present work, several different velocity profiles at the aperture are assumed, and the corresponding pressure drop for each case is calculated. The resulting theoretical predictions are compared with experimental data.

MATHEMATICAL DEVELOPMENT

We seek a theoretical relationship among viscosity, pressure drop, flow rate, and orifice diameter. The boundary value problem to be solved for the viscous flow through a sharp-edged orifice involves the Navier-Stokes equation without inertia terms as well as the equation of continuity. These equations, for an incompressible Newtonian fluid, follow respectively in vector notation:

$$\eta \nabla^2 \mathbf{V} = \nabla P \quad (1)$$

$$\nabla \cdot \mathbf{V} = 0 \quad (2)$$

These are linear partial differential equations, and a general solution can be obtained easily. In view of the geometry involved in the orifice flow, equations are transformed to cylindrical coordinates. Assuming cylindrical symmetry, eq. (1) becomes

$$\frac{1}{r} \frac{\partial}{\partial r} \left(r \frac{\partial V}{\partial r} \right) - \frac{V}{r^2} + \frac{\partial^2 V}{\partial z^2} = \frac{1}{\eta} \frac{\partial P}{\partial r} \quad (3)$$

$$\frac{1}{r} \frac{\partial}{\partial r} \left(r \frac{\partial W}{\partial r} \right) + \frac{\partial^2 W}{\partial z^2} = \frac{1}{\eta} \frac{\partial P}{\partial z} \quad (4)$$

where V and W are the radial and vertical velocity components, respectively, P is the pressure, r is radial distance from center of orifice, and z is vertical distance from orifice. Since the fluid is assumed to be highly viscous, the body force is neglected, and eq. (2) becomes

$$\frac{1}{r} \frac{\partial}{\partial r} (rV) + \frac{\partial W}{\partial z} = 0. \quad (5)$$

Equation (3) is multiplied by $rJ_1(\lambda r)$, eqs. (4) and (5) are multiplied by $rJ_0(\lambda r)$, and the products are integrated with respect to radial distance, r , from zero to infinity. Thus we have

$$\int_0^\infty r \left[\frac{1}{r} \frac{\partial}{\partial r} \left(r \frac{\partial V}{\partial r} \right) - \frac{V}{r^2} + \frac{\partial^2 V}{\partial z^2} \right] J_1(\lambda r) dr = \frac{1}{\eta} \int_0^\infty P J_1(\lambda r) dr \tag{6}$$

$$\int_0^\infty r \left[\frac{1}{r} \frac{\partial}{\partial r} \left(r \frac{\partial W}{\partial r} \right) + \frac{\partial^2 W}{\partial z^2} \right] J_0(\lambda r) dr = \frac{1}{\eta} \int_0^\infty r P J_1(\lambda r) dr \tag{7}$$

$$\int_0^\infty r \left[\frac{1}{r} \frac{\partial}{\partial r} (rV) + \frac{\partial W}{\partial z} \right] J_0(\lambda r) dr = 0 \tag{8}$$

Although the integrations are quite involved, it can be shown that the above equations can be converted respectively into the following three simultaneous ordinary differential equations:

$$\left(\frac{d^2}{dz^2} - \lambda^2 \right) R = -\frac{1}{\eta} P^* \tag{9}$$

$$\left(\frac{d^2}{dz^2} - \lambda^2 \right) Z = \frac{1}{\eta} \frac{dP^*}{dz} \tag{10}$$

$$\frac{dZ}{dz} + \lambda R = 0 \tag{11}$$

where λ is a transform variable and R , Z , and P^* are defined as follows:

$$R = \int_0^\infty r V(r, z) J_1(\lambda r) dr$$

$$Z = \int_0^\infty r W(r, z) J_0(\lambda r) dr$$

$$P^* = \int_0^\infty r P(r, z) J_0(\lambda r) dr$$

If P^* and R are eliminated from eqs. (9), (10), and (11), the following fourth-order differential equation is obtained:

$$\left(\frac{d^2}{dz^2} - \lambda^2 \right)^2 Z = 0. \tag{12}$$

A general solution of eq. (12) is

$$Z = (A + B\lambda z)e^{\lambda z} + (C + D\lambda z)e^{-\lambda z} \tag{13}$$

where A , B , C , and D are constants, but a function of the transform variable λ . These constants have to be evaluated by using the following boundary conditions:

- (a) $W(r, \infty) = 0$
- (b) $V(r, 0) = 0$.

The boundary condition (a) requires that the constants $A(\lambda)$ and $B(\lambda)$ in eq. (13) must be zero. The resulting equation is substituted in eqs. (9), (10), and (11) to obtain R and P^* as a function of the vertical distance z from the orifice as well as a function of the transform variable λ . The boundary condition (b) requires that the constants $C(\lambda)$ and $D(\lambda)$ are identical. Therefore, the final expressions for Z , R , and P^* are:

$$Z = D(\lambda)(1 + \lambda z)e^{-\lambda z} = \int_0^{\infty} rW(r,z)J_0(\lambda r)dr \quad (14)$$

$$R = \lambda D(\lambda)ze^{-\lambda z} = \int_0^{\infty} rV(r,z)J_1(\lambda r)dr \quad (15)$$

$$P^* = 2\eta\lambda D(\lambda)e^{-\lambda z} = \int_0^{\infty} rP(r,z)J_0(\lambda r)dr \quad (16)$$

The vertical and radial velocity components and the pressure can now be obtained by applying the Hankel inversion theorem⁴ to eqs. (14), (15), and (16). Hence, we have

$$W(r,z) = \int_0^{\infty} \lambda D(\lambda) (1 + \lambda z)e^{-\lambda z} J_0(\lambda r) d\lambda \quad (17)$$

$$V(r,z) = z \int_0^{\infty} \lambda^2 D(\lambda) r^{-\lambda z} J_1(\lambda r) d\lambda \quad (18)$$

$$P(r,z) = 2\eta \int_0^{\infty} \lambda^2 D(\lambda) e^{-\lambda z} J_0(\lambda r) d\lambda. \quad (19)$$

We note that velocities and pressure are expressed by integral equations with an undetermined constant or function $D(\lambda)$. The nature of the constant must be such that the integral of eq. (17) must be zero in view of the vanishing vertical velocity component along the orifice plate and far from the orifice. The fluid velocity at the orifice plate must also satisfy the following condition:

$$W(r,0) = \int_0^{\infty} \lambda D(\lambda) J_0(\lambda r) d\lambda \begin{cases} = F(r/a), & r < a \\ = 0, & r \geq a \end{cases} \quad (20)$$

It is obvious from eqs. (17) and (18) that the velocity profile at or above the orifice is a functional of the constant $D(\lambda)$. There is no rigorous way of evaluating this constant for the boundary value problem discussed here. However, this constant may be evaluated approximately by assuming a suitable velocity distribution at or above the orifice plate. Therefore, if the velocity distribution at the orifice is assumed, then the pressure difference between orifice and far away from the orifice can be calculated from eq. (19). Based on the minimum energy dissipation theorem of Helmholtz,⁵ intuitively we would think that the velocity distribution at or above the orifice is such that the total pressure drop would tend to be as small as possible for a given flow rate.

Based on the foregoing argument, we assume that the velocity distribution at the orifice can be described as

$$F\left(\frac{r}{a}\right) = K\left[1 - \left(\frac{r}{a}\right)^2\right]^n \tag{21}$$

where K and n are constants. In what follows we determine the constant $D\langle\lambda\rangle$ for several different values of n , and the resulting pressure drop is calculated by eq. (19).

For $n = 0$, the velocity profile at the orifice is flat. Since the volume flow rate is Q , we find $K = Q/\pi a^2$. The vertical velocity at the orifice is

$$W(r,0) = \int_0^\infty \lambda D\langle\lambda\rangle J_0(\lambda r) d\lambda = \frac{Q}{\pi a^2}. \tag{22}$$

By inverse transformation, we obtain the constant

$$D\langle\lambda\rangle = \frac{Q}{\pi a^2} \int_0^a r J_0(\lambda r) dr = \frac{Q}{\pi a \lambda} J_1(\lambda a). \tag{23}$$

The pressure difference between the orifice and a point far away from the orifice can now be obtained as

$$\Delta P = P_0 - P_\infty = 2\eta \frac{Q}{\pi a} \int_0^\infty \lambda J_1(\lambda a) J_0(\lambda r) d\lambda. \tag{24}$$

Equation (24) shows that the pressure is a function of radial distance in the orifice. The average at the orifice is calculated as follows:⁶

$$\begin{aligned} \overline{\Delta P} &= 4\eta \frac{Q}{\pi a^3} \int_0^a r \int_0^\infty \lambda J_1(\lambda a) J_0(\lambda r) d\lambda dr \\ &= 4\eta \frac{Q}{\pi a^3} \int_0^\infty \lambda J_1(\lambda a) \int_0^a r J_0(\lambda r) dr d\lambda \\ &= 4\eta \frac{Q}{\pi a^3} \int_0^\infty J_1^2(\xi) d\xi. \end{aligned} \tag{25}$$

The integration has been evaluated graphically and the resulting equation for the pressure becomes

$$\overline{\Delta P} = 3.31\eta \frac{Q}{a^3}. \tag{26}$$

For $n = 1/2$ and $K = 3Q/2\pi a^2$, the velocity distribution at the orifice is proportional to one-half power of the fully developed parabolic profile. The constant $D\langle\lambda\rangle$ is

$$\begin{aligned} D\langle\lambda\rangle &= \frac{3Q}{2\pi a^2} \int_0^a r \left[1 - \left(\frac{r}{a}\right)^2\right]^{1/2} J_0(\lambda r) dr \\ &= \frac{3Q}{2\pi a^2} \frac{1}{\lambda^2} \left[\frac{\sin \lambda a}{\lambda a} - \cos \lambda a \right] \end{aligned}$$

Substituting $D\langle\lambda\rangle$ into eq. (21), we find the pressure difference is

$$\begin{aligned} \Delta P &= \eta \frac{3Q}{\pi a^2} \int_0^\infty \left[\frac{\sin \lambda a}{\lambda a} - \cos \lambda a \right] J_0(\lambda r) d\lambda \\ &= \eta \frac{3Q}{\pi a^3} \cdot \begin{cases} \pi/2, & 0 \leq r < a \\ \sin^{-1}(a/r) - \frac{1}{\left[\left(\frac{r}{a}\right)^2 - 1\right]^{1/2}}, & r > a \end{cases} \end{aligned} \quad (27)$$

It should be noted that for this velocity distribution, the pressure and shearing stress at $r = a$ becomes infinite, and the pressure difference for $r < a$ is

$$\Delta P = 1.5\eta \frac{Q}{a^3}. \quad (28)$$

Finally we consider a parabolic velocity profile. For this case $n = 1$ and $K = 2Q/\pi a^2$, and

$$\begin{aligned} W(r,0) &= \int_0^\infty \lambda D\langle\lambda\rangle J_0(\lambda r) d\lambda = \frac{2Q}{\pi a^2} \left[1 - \left(\frac{r}{a}\right)^2 \right] \\ D\langle\lambda\rangle &= \frac{2Q}{\pi a^2} \int_0^a r \left[1 - \left(\frac{r}{a}\right)^2 \right] J_0(\lambda r) dr \\ &= \frac{4Q}{\pi a^2} J_2(a\lambda)/\lambda^2. \end{aligned}$$

The pressure difference now becomes

$$\begin{aligned} \Delta P &= 2\eta \frac{4Q}{\pi a^2} \int_0^\infty J_2(a\lambda) J_0(\lambda r) d\lambda \\ &= \eta \frac{16Q}{\pi a^3} \left[\frac{1}{\pi} K\left(\frac{r}{a}\right) - \frac{[1 + (r/a)^2]}{\pi(1 + r/a)} K(k) + \frac{1}{\pi} \left(1 + \frac{r}{a}\right) E(k) \right], \end{aligned} \quad (29)$$

where $K(r/a)$ and $E(k)$ are the complete elliptic integrals of the first and second kind and are defined respectively by

$$\begin{aligned} K\left(\frac{r}{a}\right) &= \frac{\pi}{2} \left[1 + \left(\frac{1}{2}\right)^2 \left(\frac{r}{a}\right)^2 + \left(\frac{1}{2} \cdot \frac{3}{4}\right)^2 \left(\frac{r}{a}\right)^4 + \dots \right] \\ E(k) &= \frac{\pi}{2} \left[1 - \left(\frac{1}{2}\right)^2 k^2 - \left(\frac{1}{2} \cdot \frac{3}{4}\right)^2 \frac{k^4}{3} - \dots \right] \end{aligned}$$

where k is defined by $k^2 = (4r/a)/(1 + r/a)^2$. The average pressure difference for this case is

$$\overline{\Delta P} = 3.825\eta \frac{Q}{a^3}. \quad (30)$$

These calculations show that for a given flow rate the pressure drop is sensitive to the assumed velocity profile at the orifice. The pressure drop goes through a minimum point as the velocity profile at the orifice changes from flat to parabolic. The exact minimum point cannot be determined analytically. It is of interest to obtain an equation for the stream function which is defined by:

$$W(r,z) = \frac{1}{r} \frac{\partial \psi}{\partial r}$$

$$V(r,z) = -\frac{1}{r} \frac{\partial \psi}{\partial z}$$

This is done by integrating eq. (18):

$$\psi = -r \int V(r,z) dz + C(r)$$

$$= r \int_0^\infty D(\lambda) e^{-\lambda z} J_1(\lambda r) (\lambda z + 1) d\lambda \tag{31}$$

where $C(r)$ is a function of r and may be assumed to be zero. The stream function at the orifice where $z = 0$ is

$$\psi(r,0) = r \int_0^\infty D(\lambda) J_1(\lambda r) d\lambda.$$

It is easy to show that eq. (31) satisfies the following relationship between vorticity and stream function

$$\omega r = \frac{\partial^2 \psi}{\partial z^2} + \frac{\partial^2 \psi}{\partial r^2} - \frac{1}{r} \frac{\partial \psi}{\partial r} \tag{32}$$

where ω is the vorticity and is defined by

$$\omega = \frac{\partial V}{\partial z} - \frac{\partial W}{\partial r}.$$

From eqs. (3) and (4) we find that vorticity must satisfy the creeping flow equation:

$$\frac{\partial^2 \omega}{\partial r^2} + \frac{1}{r} \frac{\partial \omega}{\partial r} - \frac{\omega}{r^2} + \frac{\partial^2 \omega}{\partial z^2} = 0. \tag{33}$$

Thus, we may choose an arbitrary stream function which satisfies eq. (32), but the resulting vorticity does not necessarily satisfy eq. (33).

APPARATUS

The sharp-edged orifices used in this work were made of steel, and their characteristic dimensions are shown in Table I. One side of the orifice plate was machined so as to give a 22–30° tapered edge while the flat side

TABLE I
Characteristic Dimensions of Sharp-Edged Orifices

Orifice no.	Average orifice diam, cm	Bevelled side angle, deg	Thickness of orifice plate, cm
1	0.2158	21.28	0.338
2	0.2173	33.47	0.353
3	0.2918	35.33	0.322
4	0.3155	33.40	0.320
5	0.4505	35.09	0.315
6	0.5174	29.08	0.296
7	0.4025	30.15	0.315

was ground to sharpen the orifice edge. The orifice diameter was measured with a microscope, and an average value was used for the flow rate calculation.

The sharp-edged orifice was mounted concentrically to, and at the bottom of a cylindrical fluid vessel with the tapered edge facing inside. (When the tapered edge faced outside, during flow the fluid wetted a large portion of the edge by forming a meniscus around the aperture. The pressure drop was very sensitive to the extent of wetting, and reproducibility of the data was poor.)

The vessel wall was jacketed with cooling water at constant temperature. The diameter ratio of the vessel to orifices ranged from 8.75 to 23.60. The top of the fluid vessel was connected to a constant pressure reservoir, a desired pressure was applied to the fluid using a manual pressure regulator, and the flow rate was measured when steady state was reached.

EXPERIMENTAL RESULTS AND DISCUSSION

A standard-viscosity OB Oil and a Dow-Corning #200 fluid were used to experimentally determine the orifice constant. The physical properties of OB Oil were obtained from the U.S. Bureau of Standards and are given in Table II. The viscosity of D.C. #200 fluid was measured at 25°C by using

TABLE II
Physical Properties of Standard Viscosity Oil*

Temperature, °C	Viscosity	
	Absolute (poise)	Kinematic
20	348.4	392.8
25	219.1	247.7
40	62.33	71.15

* OB Oil, lot no. 21.

a tube flow viscometer, and the result is shown in Figure 1. Figure 2 shows experimental orifice flow data obtained by using OB Oil at $19^\circ \pm 0.1^\circ\text{C}$. We see that the data can be correlated well by the following equation:

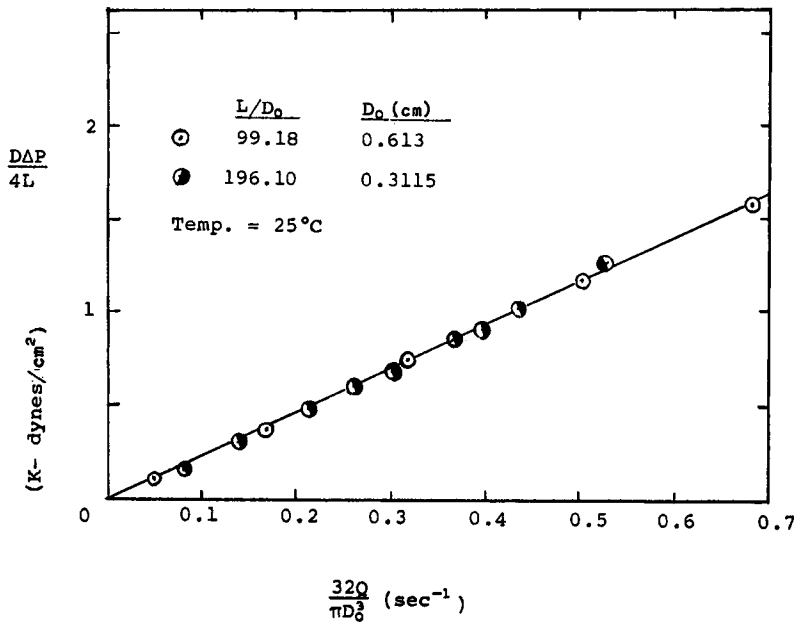


Fig. 1. Tube viscometer data of DC #200 fluid.

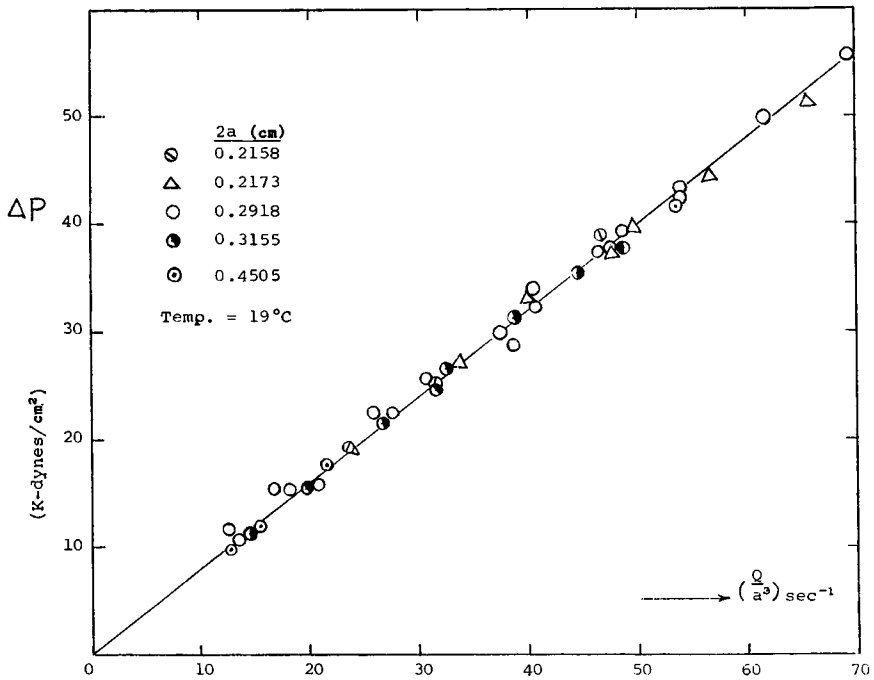


Fig. 2. Orifice flow data of OB oil (lot #21).

$$\Delta P = C_0 \eta \frac{Q}{a^3} \quad (34)$$

where C_0 is the orifice constant. The figure shows that the constant is independent of the diameter ratio of fluid vessel to orifices. Since the viscosity of OB Oil at this temperature is 428.0 poise, the constant is equal to 1.93. Figure 3 shows the orifice flow results obtained using the DC #200 fluid at 25°C. We find that the orifice constant for this fluid is 1.91. Within the experimental error the agreement between data is excellent.

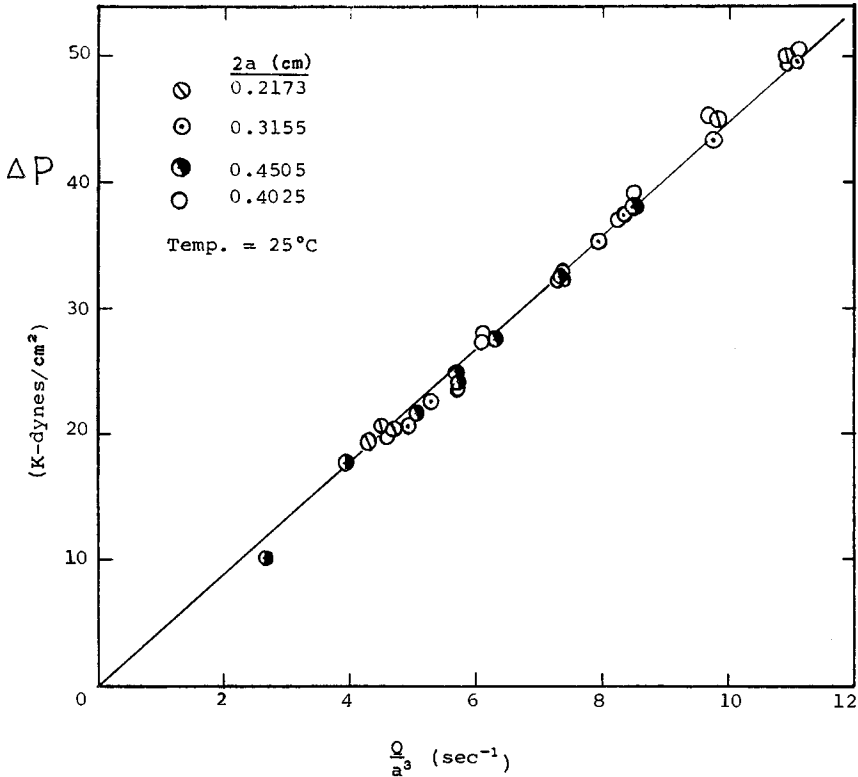


Fig. 3. Orifice flow data of DC #200 fluid.

We see that the experimentally determined orifice constant is well within the limits of the theoretical prediction. Although the velocity distribution at the orifice has not been determined experimentally, comparison of the experimental constant with the theoretical values indicates it falls somewhere between the flat and that which is proportional to the square root of a fully developed parabolic profile. However, the effect of the tapered edge on the orifice constant cannot be assessed at this time.

It is of interest to compare eq. (27) with Roscoe's solution.³ If we assume that the flow into the orifice treated in this work is equivalent to one

half of the symmetrical orifice flow and the velocity profile at the orifice is given by eq. (21) with $n = 1/2$ and $K = 3Q/2\pi a^2$, then the orifice constant for Roscoe's case should be 3. This is exactly what Roscoe's equation shows. Although the flow system treated by Weissburg² is different from this work, his final result is given here for comparison:

$$\Delta P < 3.47\eta \frac{Q}{a^3} \quad (35)$$

The empirical relationship between pressure drop and flow rate given by eq. (34) suggests that viscosity of highly concentrated suspensions with solid loadings of more than 50% by volume can be measured without the so-called wall effect. The viscosities of concentrated suspensions with various particle size distributions have been measured using an orifice flow apparatus, and the results will be published in the near future.

Notation

a	orifice radius
$A(\lambda), B(\lambda),$ $C(\lambda), D(\lambda)$	constants
C_0	orifice constant
D_0	tube diameter
J_P	Bessel function of order P
P	pressure
Q	volume flow rate at orifice
r	radial distance from center of orifice
$W(r,z)$	vertical velocity component
$V(r,z)$	radial velocity component
z	vertical distance from orifice
η	viscosity
λ	transform variable
ψ	stream function
ω	vorticity

This work is a part of the Doctoral Thesis of J. S. Chong and has been supported by the Thiokol and the Standard Oil (California) Companies. Sincere appreciation for the financial assistance is expressed.

References

1. J. S. Chong, Rheology of Concentrated Suspensions, Ph.D. Thesis, University of Utah, Salt Lake City, Utah, 1962.
2. H. L. Weissberg, *J. Phys. Fluid*, **5**, 1033 (1962).
3. R. Roscoe, *Phil. Mag.*, **40**, 338, (1949).
4. R. N. Sneddon, *Fourier Transform*, McGraw-Hill, New York, 1951.
5. L. M. Milne-Thomson, *Theoretical Hydrodynamics*, 2nd ed., Macmillan, New York, p. 510.
6. H. S. Carslow, and J. C. Jaeger, *Conduction of Heat in Solids*, 2nd ed., Oxford University Press, New York, p. 216.

Received September 15, 1970